Prev. Nutr. Food Sci. 2024;29(4):430-440
https://doi.org/10.3746/pnf.2024.29.4.430
ISSN 2287-8602

Magnolia kobus DC. Regulates Vascular Smooth Muscle Cell Proliferation by Modulating *O*-GlcNAc and MOF Expression

Hyun-Jin Na*, Jong Min Kim*, Yiseul Kim, Sang Hee Lee, and Mi-Jeong Sung

Aging and Metabolism Research Group, Food Functionality Research, Korea Food Research Institute, Wanju 55365, Korea

ABSTRACT: Vascular smooth muscle cells (VSMCs) undergo metabolic pathway transitions, including aerobic glycolysis, fatty acid oxidation, and amino acid metabolism, which are important for their function. Metabolic dysfunction in VSMCs can lead to age-related vascular diseases. *O*-GlcNAcylation, a nutrient-dependent posttranslational modification linked specifically to glucose metabolism, plays an important role in this context. *Magnolia kobus* DC. (MK), derived from the flower buds of *Magnolia biondii*, is known for its anticancer, anti-allergy, and anti-inflammatory properties. However, the role of *O*-GlcNAcylation in VSMCs under aging and the association between MK and *O*-GlcNAc remain unclear. Therefore, the present study aimed to determine the effects of *O*-GlcNAc on VSMC proliferation, along with the expression of MOF (males absent on the first, KAT8) and its correlation with the efficacy of MK. The results showed that aging and *O*-GlcNAc induction increased the expression levels of *O*-GlcNAc, *O*-GlcNAc transferase (OGT), ataxia telangiectasia mutated (ATM) protein, and MOF in mouse vascular smooth muscle cells (MOVAS) and aorta tissue. Transfection with OGT siRNA reduced the expression of MOF and OGT, indicating that OGT regulates MOF and influences cell proliferation. MK treatment reduced the expression of OGT, ATM, and MOF, which was correlated with *O*-GlcNAc levels. These findings suggest that *O*-GlcNAcylation is important for VSMC homeostasis and may be a novel target for vascular diseases. Thus, MK exhibits potential as a new drug candidate for treating vascular diseases by modulating *O*-GlcNAcylation and MOF interactions.

Keywords: aging, cardiovascular diseases, *Magnolia*, *O*-GlcNAc transferase, vascular

INTRODUCTION

Glucose-dependent metabolic pathways regulate the function and phenotype of vascular smooth muscle cells (VSMCs). These pathways have an important influence on the phenotypic transition of VSMCs under stress and aging conditions (Shi et al., 2020). *O*-GlcNAcylation, a vital posttranslational modification driven by glucose metabolism, is closely linked to cellular stress responses. It involves enzymes, including *O*-GlcNAc transferase (OGT) and *O*-GlcNAcase (Bond and Hanover, 2015). Increased *O*-GlcNAc levels often lead to enhanced protein *O*-GlcNAcylation, contributing to complications in diabetes-related cardiovascular diseases (Wright et al., 2017). *O*-GlcNAc has been observed in animal models and the arteries of patients with diabetes and is associated with worsening vascular calcification (Byon and Kim, 2020). Interestingly, *O*-GlcNAc and DNA damage response (*DDR*) genes, including ataxia telangiectasia mutated (*ATM*) and ataxia telangiectasia and Rad3-related protein (*ATR*) genes, are linked to age-related diseases, including cancer, diabetes, and cardiovascular diseases (Nikfarjam and Singh, 2023). Histone acetyltransferase MOF (males absent on the first, KAT8) activity is associated with a wide range of cellular functions, including cell cycle regulation, and DDR, which could be associated with oncogenesis and stem cell development (Singh et al., 2020). Thus, the role of *O*-GlcNAc as a nutrient sensor in VSMCs during aging is expected to greatly affect vascular health and diseases. However, the exact mechanisms remain unclear, and there is limited research focusing on OGT and MOF expression.

Magnolia kobus DC. (MK), a flower bud of *Magnolia biondii* and related plants, has been used as a traditional medicinal herb to treat rhinitis, sinusitis, nasal congestion, and sinus headaches (Shen et al., 2008). MK has been reported to exhibit anticancer properties and regulate cell proliferation, transformation, migration, inva-

Received 25 September 2024; Revised 16 October 2024; Accepted 16 October 2024; Published online 31 December 2024

Correspondence to Mi-Jeong Sung, E-mail: dulle5@kfri.re.kr
*These authors contributed equally to this work.

sion, and metastasis (Lee et al., 2015). It also exhibits a wide range of pharmacological effects, including anti-allergy, antibacterial, and anti-inflammatory activities, and antioxidant properties (Gil et al., 2022). However, the exact mechanism by which MK affects VSMCs in association with *O*-GlcNAc remains unknown, necessitating further studies to understand its potential application in the treatment of cardiovascular diseases.

In the present study, we aimed to investigate the relationship between *O*-GlcNAc expression and aging, focusing on its induction by stress related to *O*-GlcNAc in VSMCs within aortic tissues and blood vessels. Specifically, we examined the effect of *O*-GlcNAc on VSMC proliferation, along with the expression of MOF (KAT8), and its association with the efficacy of MK. We observed elevated levels of *O*-GlcNAc, DNA damage markers, and MOF in aged aortic tissue. Thiamet G (*O*-GlcNAc induction) treatment increased OGT and MOF expression, and siRNA transfection indicated that OGT and MOF regulate each other's expression, influencing cell proliferation. These findings highlight the role of *O*-GlcNAc in maintaining VSMC proliferation, which is induced by stress and aging, and suggest that MK could be a potential therapeutic target for cardiovascular diseases linked to these pathways.

MATERIALS AND METHODS

Animals

Male C57BL/6 mice were obtained from Oriental Biotechnology. The mice were maintained in rooms with a controlled temperature of 22°C±2°C and humidity of 50%±60% under a 12/12-h light/dark cycle. All animal experiments were approved by the Institutional Animal Care and Use Committee of the Korea Food Research Institute (KFRI: KFRI-M-21047) and conformed with the institutional guidelines established by the committee.

Cell line culture

Mouse vascular smooth muscle cells (MOVAS) (CRL-2797, ATCC), a mouse VSMC line, and normal human dermal fibroblasts (NHDFs) (adult, #CC-2511, Lonza) were cultured in high-glucose Dulbecco's modified Eagle medium supplemented with 10% fetal bovine serum (FBS) (Life Technologies Inc.) and 1% penicillin-streptomycin (10,000 U/mL, Sigma-Aldrich). Incubation was performed at 37°C in a humidified atmosphere with 5% CO_2, and the cells were subcultured every second day in the designed medium.

Paraffin slide immunochemistry (IHC) staining

Before proceeding with the staining protocol, paraffin slides were rehydrated with xylene and a series of ethanol concentrations (100%, 95%, 70%, and 50%) to deparaffinize them. Subsequently, they were rinsed with cold water. After the slides were deparaffinized and the heat antigen-retrieval step was performed with the unmasking solution, the slides were blocked with 5% bovine serum albumin (BSA) for 1 h and incubated overnight with the primary antibody at 4°C. Then, the samples were incubated for 2 h with secondary antibodies at 25°C, washed in phosphate-buffered saline (PBS) with Tween (PBST), mounted with VECTASHIELD, and analyzed using a Carl Zeiss Axio Imager Z2 or Olympus FV3000 microscope.

Chemical treatments

For Thiamet G treatment, the cells were treated with 300 μM of Thiamet G (Cayman Chemical) dissolved in dimethyl sulfoxide (DMSO) or DMSO alone in the culture media for 24 h at 37°C. For paraquat (PQ) treatment, the cells were treated with 300 μM of PQ (#36541, Sigma) dissolved in DMSO or DMSO alone in the culture media for 24 h at 37°C. MK cultivated in Jeollabuk-do (Korea) was purchased from a local market (Jeonju, Korea). It was ground to powder form and stored at −20°C. The ground samples were extracted with 50-fold volumes of 50% ethanol at 40°C for 24 h. The extracted samples were filtered through a Whatman No. 2 filter paper (Whatman International Limited) and concentrated using a vacuum rotary evaporator. For Thiamet G and 20 μg/mL MK treatments, the cells were treated with either 300 μM of Thiamet G or 20 μg/mL of MK, 300 μM of Thiamet G and 20 μg/mL of MK, or DMSO alone in the culture media for 24 h at 37°C. The cells were fixed after the indicated treatments.

Immunochemistry

MOVAS cells were fixed with 4% paraformaldehyde for 20 min, washed in 1% BSA, and incubated overnight with the primary antibody at 4°C. Then, the samples were incubated for 2 h with secondary antibodies at 25°C, washed in PBST, mounted with VECTASHIELD, and analyzed using a Carl Zeiss Axio Imager Z2 or Olympus FV3000 microscope.

Antisera

The primary antibodies used in this study included mouse anti-OGT (C-10) (Cat# sc-376253, 1:100 dilution; Santa Cruz Biotechnology), mouse anti-*O*-linked N-acetylglucosamine (*O*-GlcNAc) (HGAC85) (Cat# MA1-076, 1:100 dilution; Thermo Fisher Scientific), mouse anti-phospho-Histone H2A.X (Ser139) (Cat# 05-636, 1:300 dilution; Millipore), rabbit phospho-ATM/ATR Substrate Motif [(pS/pT) QG] (Cat# 6966S, 1:300 dilution; Cell Signaling), mouse anti-MOF (KAT8) (Cat# sc-271691, 1:100 dilution; Santa Cruz Biotechnology), rabbit anti-Ki-67

(Cat# ab15580, 1:100 dilution; Abcam), mouse anti-Ki-67 (SP6; Cat# MA5-14520, 1:50 dilution; Thermo Fisher Scientific), and rabbit anti-actin (Cell Signaling, 1:300 dilution).

RNAi transfection

Prior to the experiment, 3 to 50,000 cells/well were added to a six-well plate in a culture medium. On the day of transfection, the cells were washed once with sterile PBS, and the culture medium was added with the transfection reagents (Lipofectamine™ RNAiMAX, Cat#:137 78150; Thermo). For transfection with Lipofectamine RNAiMAX, the culture medium was replaced with 100 μL of Opti-MEM (1×) plus GlutaMAX and 5% FBS before adding Lipofectamine RNAiMAX. MOF siRNA (#ID: 180049, Thermo) and OGT siRNA (#ID: 173150, Thermo) were transfected.

Cell viability assay

Cell survival was determined using a Cell Counting Kit-8 (CCK-8) assay kit (Dongin LS Co.) in accordance with the manufacturer's protocols. MOVAS cells were transfected with OGT and MOF siRNAs (200 or 400 pmol/well) using Lipofectamine RNAiMAX (Invitrogen). After 48 h of transfection, 10 μL of CCK-8 was added to wells containing cells in 100 μL of media. Fluorescent signals were detected at 450 nm using a SpectraMAX 190 fluorescence microplate reader (Molecular Devices).

Western blot analysis

MOVAS cells were lysed in radioimmunoprecipitation assay buffer containing protease and phosphatase inhibitors for protein extraction and subsequently centrifuged. The protein concentration of the extracts was measured using bicinchoninic acid protein assay (Thermo Fisher Scientific). The proteins were separated via sodium dodecyl sulfate-polyacrylamide gel electrophoresis and subsequently transferred onto polyvinylidene difluoride (PVDF) membranes (Bio-Rad). The PVDF membranes were blocked with 5% BSA and incubated overnight with primary antibodies. Thereafter, the membranes were incubated with anti-rabbit secondary antibodies. Finally, the signals were visualized using an image analyzer (ChemiDoc™ XRS+System, Bio-Rad Laboratories), and densitometry was performed using ImageJ software (National Institutes of Health).

Measurement of *O*-GlcNAc, H2AX, OGT, and MOF fluorescence

The mean fluorescence of *O*-GlcNAc, H2AX, OGT, and MOF was measured in accordance with the method of Na et al. (2020). The images displaying the fluorescence intensity of *O*-GlcNAc, H2AX, OGT, and MOF staining were captured with the same exposure time in each experiment and measured by quantifying the fluorescence level (IHC staining) in MOVAS and NHDF cell lines (Ki-67 positive cells) and aorta tissue normalized to the nearby background using ImageJ-Fiji (NIH). The mean fluorescence was analyzed after excluding the mean of the background region (from two spots). "n" denotes the number of cells.

Antioxidant capacity: total phenolic content and total flavonoid content

The total phenolic content (TPC) of MK was assessed in accordance with the Folin-Ciocalteu method (Kim et al., 2003a). The sample mixed with Folin-Ciocalteu reagent and Na_2CO_3 was incubated at 25°C for 2 h. The absorbance of the reactant was measured at 760 nm using a spectrophotometer (Libra S32PC, Biochrom Ltd.). The TPC was calculated as mg of gallic acid equivalent (GAE)/g.

The total flavonoid content (TFC) of MK was measured in accordance with a previously described method with modifications (Abeysinghe et al., 2007). The sample was mixed with diethylene glycol and NaOH and incubated at 30°C for 1 h. The absorbance of the reactant was measured at 420 nm using a spectrophotometer (Libra S32PC). The TFC was calculated as mg of rutin equivalent (RE)/g.

Antioxidant capacity measurement [2,2′-azino-bis(3-ethylbenzothiazoline-6-sulfonic acid) (ABTS), 1,1-diphenyl-2-picrylhydrazyl (DPPH)]

To evaluate the antioxidant capacity of MK, ABTS and DPPH radical scavenging assays were conducted (Chang et al., 2001). To measure the ABTS radical scavenging activity, the sample was mixed with ABTS, where the absorbance was set to 0.70±0.02 at 734 nm (pH 7.4), and reacted at 37°C for 10 min. The absorbance of the reactant was measured at 734 nm using a spectrophotometer (Libra S32PC). To measure the DPPH radical scavenging activity, the sample was mixed with 0.1 mM DPPH in 80% methanol, where the absorbance was set to 1.00±0.02 at 517 nm, and reacted at 25°C for 30 min in a dark room. The absorbance of the reactant was measured at 517 nm using a spectrophotometer (Libra S32PC) (Kim et al., 2003a). The results of the ABTS and DPPH radical scavenging assays are presented as IC_{50} value (μg/mL). To measure the inhibitory effect of MK against lipid peroxide, mouse cerebral tissue, which is rich in unsaturated fatty acids, was collected and homogenized with 20 mM Tris hydrochloride buffer (pH 7.4). These homogenized tissues were centrifuged at 12,000 *g* for 15 min at 4°C, and the supernatant was used in subsequent experiments. The sample was reacted with the cerebral supernatant, 10 μM of $FeSO_4$, and 0.1 mM ascorbic acid and then incubated at 37°C for 1 h. After incubation, the

reactant was mixed with 30% trichloroacetic acid and 1% thiobarbituric acid and heated at 80°C for 20 min. The absorbance of the reactant was measured at 532 nm using a spectrophotometer (Libra S32PC) (Benzie and Strain, 1996). The results of the inhibitory activity against malondialdehyde (MDA) are presented as IC_{50} value (μg/mL). To evaluate the ferric ion reducing antioxidant power (FRAP) of MK, the sample was reacted with 300 mM sodium acetate buffer (pH 3.6), 10 mM 2,4,6-tri(2-pyridyl)-1,3,5-triazine, and 20 mM $FeCl_3$ at 37°C for 15 min. After incubation, the absorbance of the reactant was measured at 593 nm using a spectrophotometer (Libra S32PC). The FRAP was calculated as mg of Fe(II)/g. Moreover, a standard curve was measured using vitamin C as a positive control, and the vitamin C equivalent antioxidant capacity (VCEAC, mg of VCE/100 g dry weight) was calculated.

Statistical analysis

Data representation and statistical analysis were performed using GraphPad Prism software. Statistical analysis was performed using a *t*-test and multiple comparisons with one-way analysis of variance. All experiments were replicated thrice.

RESULTS

O-GlcNAc, OGT, MOF(KAT8), and ATM levels were elevated in aged aortic tissues

Cardiovascular disease has serious clinical consequences and is implicated in several diseases, including aging and diabetes (Pernomian et al., 2013). *O*-GlcNAcylation is induced in stress and cancer (Lee et al., 2021). The expression of DDR-related genes, including *ATM* and *ATR*, is increased in response to stress, aging, cancer, and cardiovascular diseases (Nikfarjam and Singh, 2023). MOF (KAT8) may be involved in transcriptional activation and is associated with ATM function (Singh et al., 2020). Thus, we aimed to determine whether OGT and MOF expression is changed in aged vascular tissue. We used tissues from young (6 months) and old C57BL/6 mice (21 months) to determine whether the expression of *O*-GlcNAc, OGT, ATM, and MOF is increased in aged vascular aortic tissues. The expression of OGT (Fig. 1B and 1C), *O*-GlcNAc (Fig. 1D and 1E), ATM (Fig. 1F and 1G), H2AX (Fig. 1H and 1I), and MOF (Fig. 1J and 1K) was increased in vascular aortic tissue cells, and the aged vascular aortic tissue was thickened compared with young mouse tissue (Fig. 1). The expression of OGT, H2AX, MOF, and *O*-GlcNAc was increased by a minimum of 50% and maximum of 200% in old tissue than in young tissue (Fig. 1). This finding indicates that the levels of OGT, H2AX, MOF, and *O*-GlcNAc increase with age and may be associated with the homeostasis of tissues thickened by aging.

OGT and MOF regulated cell proliferation in the MOVAS cell line

Our results indicate that when ATM and OGT were strongly expressed, the expression of MOF also increased (Fig. 1). Therefore, we determined whether ATM and MOF expression levels were associated with cell homeostasis using the OGT siRNA transfection system. The results of Western blot analysis showed that OGT or MOF protein levels were reduced by siRNA transfection of OGT/MOF compared with the control (Fig. 2A and 2B). OGT or MOF siRNA transfection coupled with Thiamet G treatment in the MOVAS cell line resulted in decreased cell viability (Fig. 2C and 2D). Our data also revealed that the cell numbers decreased because of the siRNA transfection of OGT/MOF compared with the control in the NHDF cell line (Fig. 2E). The OGT levels were increased because of Thiamet G treatment but did not increase upon OGT siRNA transfection coupled with Thiamet G treatment in NHDF cells (Fig. 2F and 2G). The MOF level of Ki-67-positive cells increased with Thiamet G treatment but did not increase following OGT or MOF siRNA transfection and treatment with Thiamet G in the MOVAS cell line (Fig. 3). Our data indicated that OGT and MOF are closely associated with DDR. Thus, OGT and MOF can be controlled and are essential for stress responses in VSMCs and fibroblast proliferation.

MK regulated the increased levels of *O*-GlcNAc, OGT, MOF, and ATM induced by Thiamet G treatment

Next, we examined whether the expression of *O*-GlcNAc, OGT, ATM, and MOF, which increased because of *O*-GlcNAc induction stress, decreased after MK treatment. MK, a member of *Magnolia* spp., has anticancer, anti-allergy, and anti-inflammatory properties (Lee et al., 2015). The cell viability increased with Thiamet G treatment and decreased with MK treatment (Fig. 4A). Fig. 4B shows the OGT and MOF protein levels induced by Thiamet G treatment in MOVAS cells and after MK treatment. The results showed that the increased *O*-GlcNAc levels induced by Thiamet G treatment decreased upon treatment with MK and Thiamet G in MOVAS cells (Fig. 4C and 4D). Moreover, the OGT levels, which were upregulated after Thiamet G treatment, decreased upon treatment with MK and Thiamet G in MOVAS cells compared with those in cells treated with Thiamet G alone (Fig. 4E and 4F). When Thiamet G was used in conjunction with MK, the MOF and ATM levels were reduced compared with those observed after Thiamet G treatment alone (Fig. 5). Therefore, it can be concluded that MK regulates smooth muscle and fibroblast cell proliferation by controlling *O*-GlcNAc, OGT, ATM, and MOF levels. To

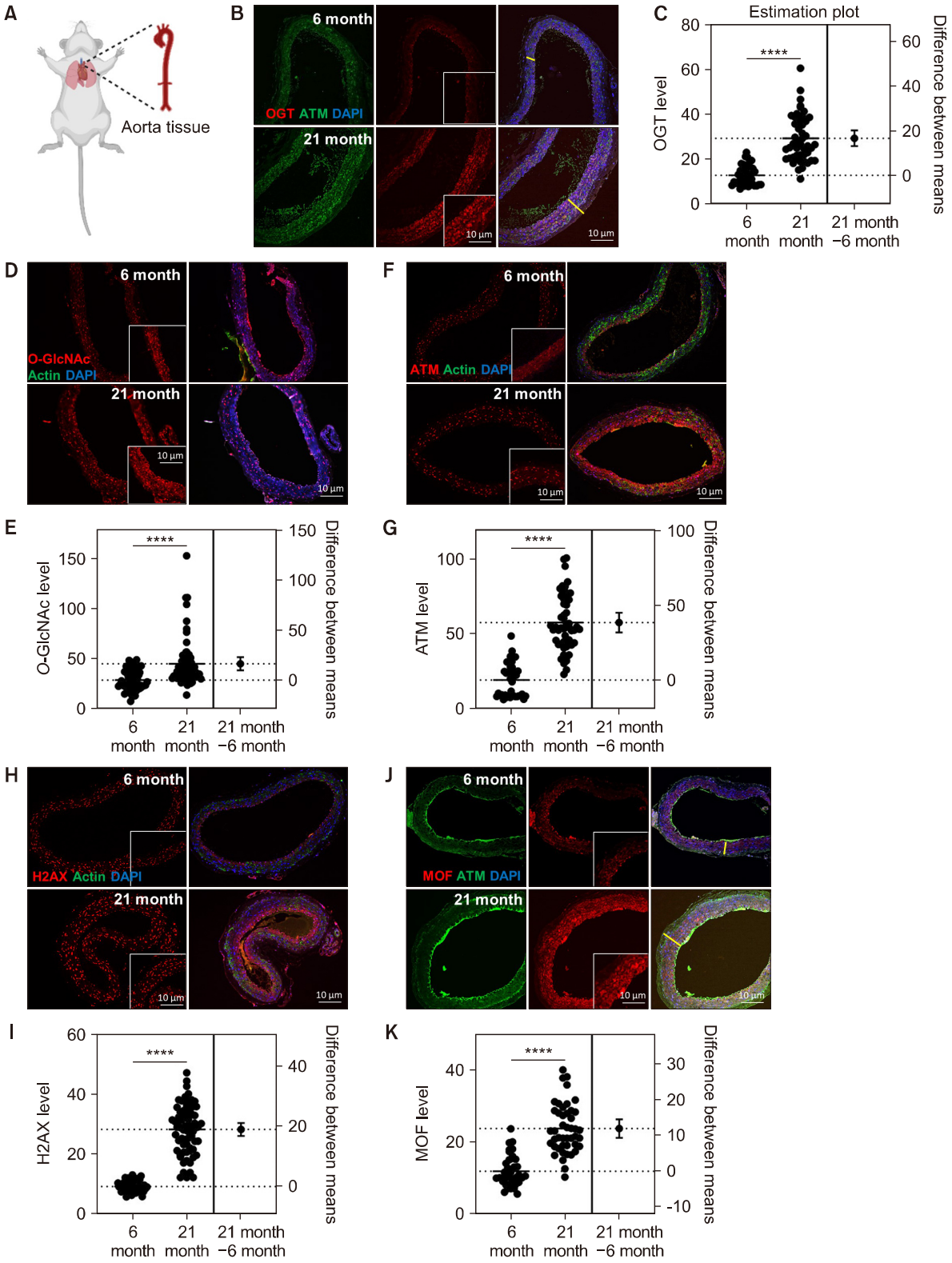

Fig. 1. *O*-GlcNAc, *O*-GlcNAc transferase (OGT), MOF (KAT8), and ATM levels were elevated in aged aorta tissues. (A) Illustration of mouse aorta tissue. (B) Immunofluorescence staining of OGT (red) and ATM (pS/Tq, green), which indicates ATM/ATR activity in young (6 months) and old (21 months) mouse aorta tissue. (C) Quantification of OGT mean fluorescence in young (n=39) and old mice (n=49). (D) Immunofluorescence staining of *O*-GlcNAc (red) and actin (green). (E) Quantification of *O*-GlcNAc mean fluorescence in young (n=63) and old mice (n=63). (F) Immunofluorescence staining of ATM (pS/Tq, red) and actin (green). (G) Quantification of ATM mean fluorescence in young (n=39) and old mice (n=53). (H) Immunofluorescence staining of H2AX (red) and actin (green). (I) Quantification of ATM mean fluorescence in young (n=56) and old mice (n=69). (J) Immunofluorescence staining of MOF (red) and ATM (pS/Tq, green), which indicates ATM/ATR activity. (K) Quantification of MOF mean fluorescence in young (n=35) and old mice (n=45). The white line indicates the width of the aorta. The insert in each panel is an enlarged image of the area where the line is displayed. Data are presented as the mean±SD. ****P<0.0001. ns, non-significant. ATM, ataxia telangiectasia mutated.

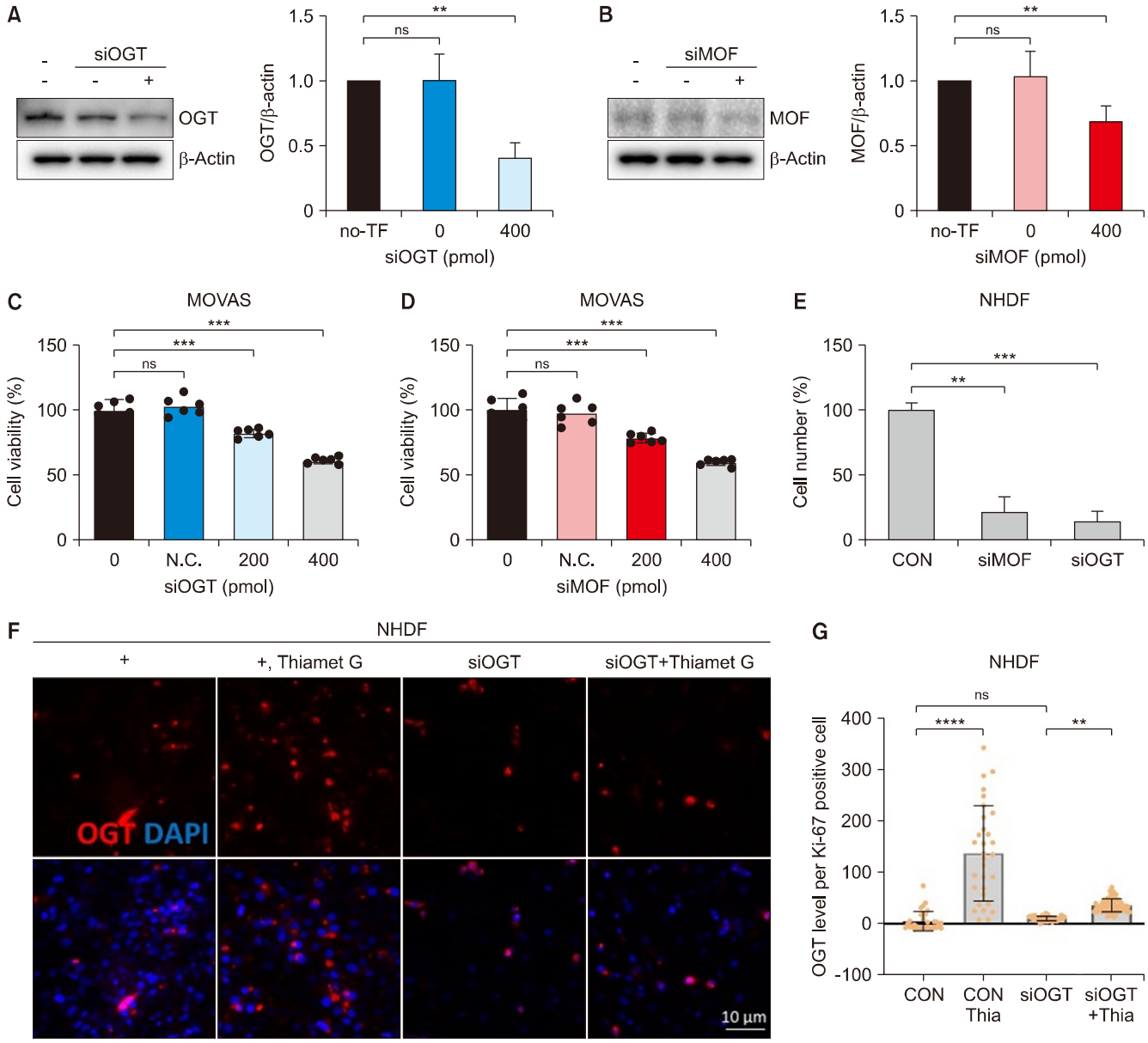

Fig. 2. OGT and MOF regulate the proliferation of MOVAS and fibroblast cell lines. (A) Effects of OGT siRNA transfection and (B) MOF siRNA transfection. (C) Quantification of cell viability in siOGT-transfected MOVAS cells. (D) Quantification of cell viability in siMOF-transfected MOVAS cells. (E) Quantification of the cell number in siOGT- or siMOF-transfected NHDF cell line. (F) Immunofluorescence staining of OGT (red) in the NHDF cell line or siOGT-transfected NHDF cells with/without Thiamet G treatment. (G) Quantification of OGT (red) in the NHDF cell line or siOGT-transfected NHDF cells with/without Thiamet G (Thia) treatment. CON, n=32; CON+Thia, n=31; siOGT, n=62; siOGT+Thia, n=70. Data are presented as the mean±SD. $^{**}P<0.01$, $^{***}P<0.001$, $^{****}P<0.0001$. ns, non-significant. n indicates the cell numbers. OGT, *O*-GlcNAc transferase; TF, transfection; MOF, males absent on the first; MOVAS, mouse vascular smooth muscle cells; N.C., negative control; CON, control; NHDF, normal human dermal fibroblast.

confirm whether MK has antioxidant activity, the TPC, TFC, ABTS, and DPPH radical scavenging activities; MDA inhibitory effect; and FRAP were evaluated (Table 1). MK exhibited considerable TPC and TFC levels and was presumed to contain a large amount of bioactive compounds. Moreover, MK exhibited significant radical scavenging activity, inhibitory effects against lipid peroxidation, and ferric ion reducing effects. These results indicate that MK may have an excellent effect on aging- and stress-induced VSMC dysfunction.

DISCUSSION

Glucose-dependent metabolism affects the behavior of VSMCs, with high-glucose levels activating signaling pathways, including JAK-STAT3/Pim-1, which contributes to the proliferation of VSMCs (Wang et al., 2017). A lower degree of proliferation was observed in VSMCs derived from pulmonary arteries with an enhanced glycolysis/glucose oxidation ratio (Chiong et al., 2013). Our data indicate that *O*-GlcNAc levels were elevated in the tissue of male mice (Fig. 1). *O*-GlcNAcylation, a nutrient-driv-

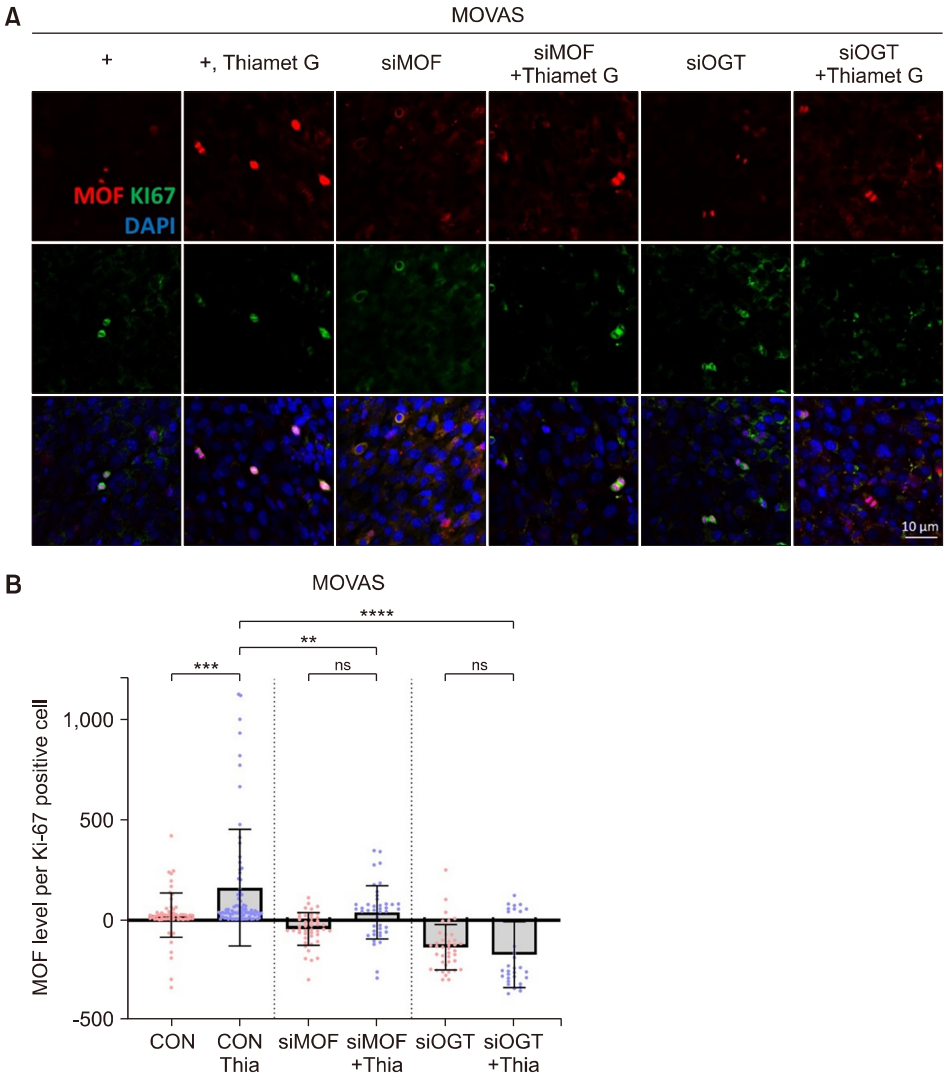

Fig. 3. *O*-GlcNAc transferase (OGT) regulates the MOF levels. (A) Immunofluorescence staining of MOF (red) and Ki-67 (green) in MOVAS cells or siMOF-transfected MOVAS or siOGT-transfected MOVAS cells with/without Thiamet G (Thia). (B) Quantification of MOF mean fluorescence. CON, n=63; CON+Thia, n=82; siOGT, n=44; siOGT+Thia, n=42; siMOF, n=40; and siMOF+Thia (n=31). Data are presented as the mean±SD. $^{**}P<0.01$, $^{***}P<0.001$, $^{****}P<0.0001$. ns, non-significant. n indicates the cell numbers. CON, control; MOF, males absent on the first; MOVAS, mouse vascular smooth muscle cells.

en posttranslational modification, is crucial for normal cellular function and homeostasis in the cardiovascular system (Narayanan et al., 2023). When vascular compliance is impaired, studies indicate that increased *O*-GlcNAcylation in diabetes leads to AKT activation and upregulation of Runx2 expression, thereby promoting VSMC calcification (Heath et al., 2014). *O*-GlcNAc regulates VSMCs in conjunction with several other factors. Our findings demonstrated that nutrient-driven increases in *O*-GlcNAc and OGT levels are correlated with high *O*-GlcNAc in VSMCs, promoting proliferation and activating *DDR* genes, including *H2AX*, *ATM*, and *ATR*. This highlights a significant association between stress and VSMC-related diseases, suggesting potential therapeutic targets for managing vascular pathologies.

As the enzyme responsible for adding *O*-GlcNAc moieties to proteins, OGT is important in modulating reactive oxygen species levels in stem and progenitor cells under high-glucose conditions. These findings underscore *O*-GlcNAcylation as an important determinant of DDR and highlight its potential therapeutic implications in conditions characterized by metabolic reprograming and genomic instability. MOF, which is an acetyltransferase enzyme, is implicated in various cellular processes, including cell cycle regulation and DNA repair, particularly through its interaction with ATM. MOF can acetylate ATM, modulating its activity in cell cycle checkpoint control, and p53 (Li et al., 2010), directing cells toward apoptosis (Sykes et al., 2006; Gupta et al., 2014). MOF and ATM levels increased with elevated *O*-GlcNAc levels, suggesting a regulatory connection between *O*-GlcNAcylation, MOF, and ATM in cellular proliferation, including VSMCs (Fig. 2). This finding indicates that OGT and MOF are closely associated with DDR. Furthermore, experimental manipulation using siRNA targeting OGT or MOF demonstrated the reciprocal downregulation of these proteins, indicating their interdependence and collective influence on VSMC proliferation (Fig. 2 and 3). Thus, the interconnected roles of *O*-GlcNAcylation, OGT, MOF, and ATM underscore their importance in maintaining cellular proliferation under stress conditions.

Magnolia exerts anticancer effects by regulating the proliferation, transformation, migration, invasion, and metastasis of cancer cells (Lee et al., 2015). It also exerts a

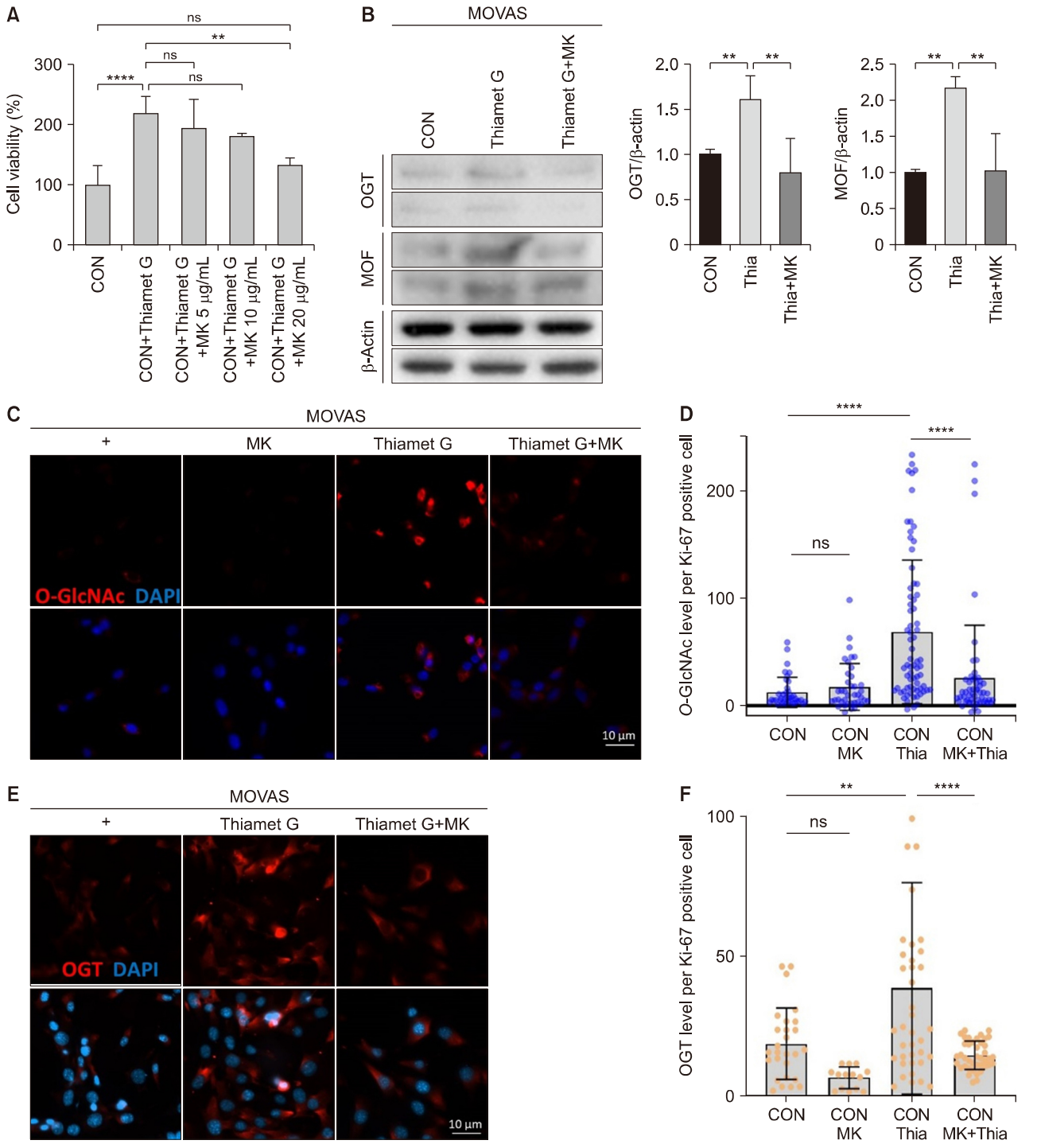

Fig. 4. Magnolia regulated the levels of *O*-GlcNAc, OGT, and MOF induced by Thiamet G in MOVAS cells. (A) Quantification of cell viability in MOVAS cells treated with 300 μM of Thiamet G (Thia) or Thiamet G + 5, 10, and 20 μg/mL of MK for 24 h. (B) Western blot analysis using antibodies against OGT, MOF, and beta-actin in MOVAS cells treated with 300 μM of Thiamet G or 300 μM of Thiamet G + 20 μg/mL of MK for 24 h. (C) Immunofluorescence staining images of *O*-GlcNAc (red) in untreated MOVAS cells and MOVAS cells treated with 20 μg/mL of MK, 300 μM of Thiamet G, and 20 μg/mL of MK + 300 μM of Thiamet G. (D) Quantification of *O*-GlcNAc mean fluorescence. (E) Immunofluorescence staining images of OGT (red) in untreated MOVAS cells and MOVAS cells treated with 300 μM of Thiamet G and 20 μg/mL of MK + 300 μM of Thiamet G. (F) Quantification of OGT mean fluorescence. CON, n=29; CON+MK, n=17; CON+Thia, n=41; CON+Thia+MK, n=43. Data are presented as the mean±SD. $^{**}P<0.01$, $^{****}P<0.0001$. ns, non-significant. n indicates the cell numbers. CON, control; OGT, *O*-GlcNAc transferase; MOF, males absent on the first; MOVAS, mouse vascular smooth muscle cells; MK, *Magnolia kobus* DC.

wide range of pharmacological effects, including anti-allergy, antibacterial, and anti-inflammatory activities, and regulates antioxidant activity (Tanaka et al., 2002; Ma et al., 2019). Our data indicated the antioxidant effect of MK through the VCEAC (Table 1). In addition, Magnolia induces caspase-dependent mast cell apoptosis, and its

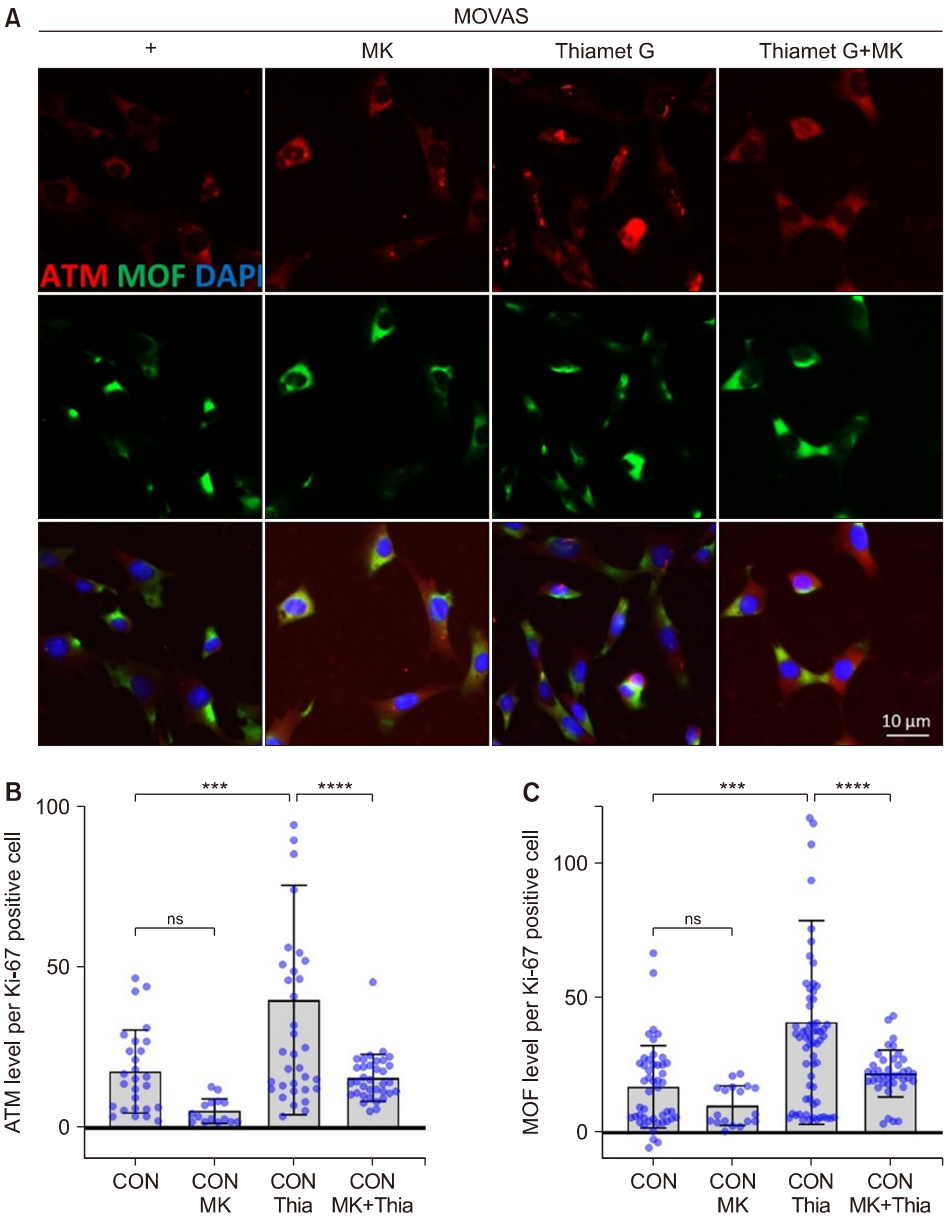

Fig. 5. MK regulated ATM and MOF levels. (A) Immunofluorescence staining images of ATM (red) and MOF (green) in untreated cells and cells treated with Thiamet G (Thia) and MK + Thiamet G. (B) Quantification of ATM mean fluorescence. CON, n=29; CON+MK, n=17; CON+Thia, n=37; CON+Thia+MK, n=36. (C) Quantification of MOF mean fluorescence. CON, n=47; CON+MK, n=18; CON+Thia, n=65; CON+Thia+MK, n=39. Data are presented as the mean±SD. $^{**}P<0.01$, $^{***}P<0.001$, $^{****}P<0.0001$. ns, non-significant. n indicates the cell numbers. ATM, ataxia telangiectasia mutated; MOF, males absent on the first; CON, control; MOVAS, mouse vascular smooth muscle cells; MK, *Magnolia kobus* DC.

Table 1. Antioxidant capacity of *Magnolia kobus* DC. (MK) extract

	TPC	TFC	ABTS	DPPH	MDA	FRAP
MK	136.12±6.25	79.31±1.12	232.25±9.14	321.06±5.18	14.09±0.19	60.78±6.12
VCEAC	–	–	154.21±8.6	111.27±10.2	183.24±15.15	205.22±13.27

The results shown are mean±SD (n=3).
TPC, total phenolic content; TFC, total flavonoid content; ABTS, 2,2-azino-bis(3-ethylbenzothiazoline-6-sulfonic acid) radical scavenging activity; DPPH, 1,1-diphenyl-2-picrylhydrazyl radical scavenging activity; MDA, malondialdehyde inhibitory effect; FRAP, ferric ion reducing antioxidant power; VCEAC, vitamin C equivalent antioxidant capacity.
The results of TPC and TFC are presented as mg of gallic acid equivalent (GAE)/g and mg of rutin equivalent (RE)/g, respectively. The results of ABTS, DPPH, and MDA are presented as IC_{50} value (μg/mL). The results of FRAP are presented as mg of Fe(II) mg/g. The results of VCEAC are presented as mg of VCE/100 g dry weight.

clinical effects are related to its pharmacological efficacy in regulating mast cell apoptosis (Kim et al., 2003b). MK alleviates oxidative stress, prevents inflammation and calcification, and supports cellular and mitochondrial function, especially under stress conditions (Jung et al., 1997; Wang et al., 2014; Lee et al., 2023). These effects play a pivotal role in maintaining the proliferation of VSMCs. Antioxidants are well-known molecules with numerous biological functions. Although they primarily serve as reducing agents and cofactors for various enzymatic reactions, emerging evidence suggests that they might influence glucose metabolism and associated oxi-

dative stress-related signaling pathways (Peng et al., 2022). The role of antioxidants, such as MK, could affect the flux through the hexosamine biosynthesis pathway (HBP), thereby influencing *O*-GlcNAcylation. Specifically, the HBP, which produces uridine diphosphate-N-acetyl glucosamine, is sensitive to changes in the glucose flux (Olson et al., 2020). The hypothesis that MK has the ability to modulate *O*-GlcNAc can be inferred from the association between the bioactive compounds present in MK and the pathways related to *O*-GlcNAc. *O*-GlcNAc is known to respond dynamically to oxidative stress (Chen et al., 2018), with increased *O*-GlcNAcylation acting as a protective mechanism in stressed cells. The established antioxidative stress properties of MK are important here (Table 1) (Wang et al., 2014) as cells undergoing oxidative stress often exhibit elevated *O*-GlcNAc to protect against damage. MK's ability to mitigate oxidative stress could suggest that it modulates *O*-GlcNAc levels, possibly by enhancing or normalizing the stress response pathways that involve this modification. Moreover, MK might modulate signaling pathways that are sensitive to *O*-GlcNAc under oxidative conditions. Although the known effects of MK in cancer, inflammation, and neuroprotection are not direct evidence of its role in *O*-GlcNAc, there is a potential intersection of its bioactive components with pathways involving this critical protein modification. In addition, the hypothesis that MK has the ability to modulate *O*-GlcNAc requires an in-depth analysis of the bioactive compounds present in MK and their biological effects that may intersect with the pathways involved in *O*-GlcNAcylation.

In our study, the aging and induction of *O*-GlcNAcylation using Thiamet G led to increased OGT, ATM, and MOF levels in MOVAS cells and aged aortas. These proteins are crucial in regulating cellular functions, including proliferation. Specifically, our data indicated that the expression of OGT and MOF influenced MOVAS cell proliferation, suggesting their role in maintaining tissue homeostasis under *O*-GlcNAc induction and aging conditions. The ability of MK to modulate these factors makes it a promising candidate for cardiovascular disease treatment, particularly in conditions characterized by *O*-GlcNAc dysregulation, including nutrient-dependent diabetes and obesity. However, there is a possibility of different efficacy depending on individual differences, concentration, and treatment period. Thus, in-depth studies on the concentration and treatment period are needed to determine the efficacy of MK. Further research into these pathways in other vascular cell types would expand our understanding of how *O*-GlcNAc and its regulatory proteins contribute to cardiovascular diseases. Ultimately, targeting *O*-GlcNAc regulation, possibly through compounds such as MK, holds potential as a therapeutic strategy for managing cardiovascular diseases associated with aging.

FUNDING

This research was supported by the Main Research Program (E0210102) of the Korea Food Research Institute.

AUTHOR DISCLOSURE STATEMENT

The authors declare no conflict of interest.

AUTHOR CONTRIBUTIONS

Concept and design: HJN, MJS. Analysis and interpretation: HJN, YK, JMK. Data collection: HJN, YK, MJS. Writing the article: HJN, MJS. Critical revision of the article: HJN, MJS. Final approval of the article: all authors. Statistical analysis: HJN, YK, JMK. Obtained funding: MJS. Overall responsibility: HJN, MJS.

REFERENCES

Abeysinghe DC, Li X, Sun CD, Zhang WS, Zhou CH, Chen KS. Bioactive compounds and antioxidant capacities in different edible tissues of citrus fruit of four species. Food Chem. 2007. 104:1338-1344. https://doi.org/10.1016/j.foodchem.2007.01.047

Benzie IF, Strain JJ. The ferric reducing ability of plasma (FRAP) as a measure of "antioxidant power": The FRAP assay. Anal Biochem. 1996. 239:70-76. https://doi.org/10.1006/abio.1996.0292

Bond MR, Hanover JA. A little sugar goes a long way: The cell biology of O-GlcNAc. J Cell Biol. 2015. 208:869-880. https://doi.org/10.1083/jcb.201501101

Byon CH, Kim SW. Regulatory effects of O-GlcNAcylation in vascular smooth muscle cells on diabetic vasculopathy. J Lipid Atheroscler. 2020. 9:243-254. https://doi.org/10.12997/jla.2020.9.2.243

Chang ST, Wu JH, Wang SY, Kang PL, Yang NS, Shyur LF. Antioxidant activity of extracts from *Acacia confusa* bark and heartwood. J Agric Food Chem. 2001. 49:3420-3424. https://doi.org/10.1021/jf0100907

Chen PH, Chi JT, Boyce M. Functional crosstalk among oxidative stress and O-GlcNAc signaling pathways. Glycobiology. 2018. 28:556-564. https://doi.org/10.1093/glycob/cwy027

Chiong M, Morales P, Torres G, Gutiérrez T, García L, Ibacache M, et al. Influence of glucose metabolism on vascular smooth muscle cell proliferation. Vasa. 2013. 42:8-16. https://doi.org/10.1024/0301-1526/a000243

Gil TY, Jin BR, Cha YY, An HJ. *Magnoliae flos* downregulated lipopolysaccharide-induced inflammatory responses via NF-κB/ERK-JNK MAPK/STAT3 pathways. Mediators Inflamm. 2022. 2022:6281892. https://doi.org/10.1155/2022/6281892

Gupta A, Hunt CR, Hegde ML, Chakraborty S, Chakraborty S, Udayakumar D, et al. MOF phosphorylation by ATM regulates 53BP1-mediated double-strand break repair pathway choice. Cell Rep. 2014. 8:177-189. https://doi.org/10.1016/j.celrep.

2014.05.044
Heath JM, Sun Y, Yuan K, Bradley WE, Litovsky S, Dell'Italia LJ, et al. Activation of AKT by O-linked N-acetylglucosamine induces vascular calcification in diabetes mellitus. Circ Res. 2014. 114:1094-1102. https://doi.org/10.1161/circresaha.114.302968
Jung KY, Lee IS, Oh SR, Kim DS, Lee HK. Lignans with platelet activating factor antagonist activity from *Schisandra chinensis* (Turcz.) Baill. Phytomedicine. 1997. 4:229-231. https://doi.org/10.1016/s0944-7113(97)80072-4
Kim DO, Jeong SW, Lee CY. Antioxidant capacity of phenolic phytochemicals from various cultivars of plums. Food Chem. 2003a. 81:321-326. https://doi.org/10.1016/S0308-8146(02)00423-5
Kim GC, Lee SG, Park BS, Kim JY, Song YS, Kim JM, et al. Magnoliae flos induces apoptosis of RBL-2H3 cells via mitochondria and caspase. Int Arch Allergy Immunol. 2003b. 131:101-110. https://doi.org/10.1159/000070925
Lee CJ, Lee MH, Yoo SM, Choi KI, Song JH, Jang JH, et al. Magnolin inhibits cell migration and invasion by targeting the ERKs/RSK2 signaling pathway. BMC Cancer. 2015. 15:576. https://doi.org/10.1186/s12885-015-1580-7
Lee HJ, Lee SJ, Lee SK, Choi BK, Lee DR. *Magnolia kobus* extract inhibits periodontitis-inducing mediators in *Porphyromonas gingivalis* lipopolysaccharide-activated RAW 264.7 cells. Curr Issues Mol Biol. 2023. 45:538-554. https://doi.org/10.3390/cimb45010036
Lee JB, Pyo KH, Kim HR. Role and function of O-GlcNAcylation in cancer. Cancers. 2021. 13:5365. https://doi.org/10.3390/cancers13215365
Li X, Corsa CA, Pan PW, Wu L, Ferguson D, Yu X, et al. MOF and H4 K16 acetylation play important roles in DNA damage repair by modulating recruitment of DNA damage repair protein Mdc1. Mol Cell Biol. 2010. 30:5335-5347. https://doi.org/10.1128/mcb.00350-10
Ma P, Che D, Zhao T, Zhang Y, Li C, An H, et al. Magnolin inhibits IgE/Ag-induced allergy *in vivo* and *in vitro*. Int Immunopharmacol. 2019. 76:105867. https://doi.org/10.1016/j.intimp.2019.105867
Na HJ, Akan I, Abramowitz LK, Hanover JA. Nutrient-driven *O*-GlcNAcylation controls DNA damage repair signaling and stem/progenitor cell homeostasis. Cell Rep. 2020. 31:107632. https://doi.org/10.1016/j.celrep.2020.107632
Narayanan B, Sinha P, Henry R, Reeves RA, Paolocci N, Kohr MJ, et al. Cardioprotective O-GlcNAc signaling is elevated in murine female hearts via enhanced O-GlcNAc transferase activity. J Biol Chem. 2023. 299:105447. https://doi.org/10.1016/j.jbc.2023.105447
Nikfarjam S, Singh KK. DNA damage response signaling: A common link between cancer and cardiovascular diseases. Cancer Med. 2023. 12:4380-4404. https://doi.org/10.1002/cam4.5274
Olson AK, Bouchard B, Zhu WZ, Chatham JC, Des Rosiers C. First characterization of glucose flux through the hexosamine biosynthesis pathway (HBP) in *ex vivo* mouse heart. J Biol Chem. 2020. 295:2018-2033. https://doi.org/10.1074/jbc.RA119.010565
Peng ML, Fu Y, Wu CW, Zhang Y, Ren H, Zhou SS. Signaling pathways related to oxidative stress in diabetic cardiomyopathy. Front Endocrinol. 2022. 13:907757. https://doi.org/10.3389/fendo.2022.907757
Pernomian L, Gomes MS, Corrêa FM, Restini CB, Ramalho LN, de Oliveira AM. Diabetes confers a vasoprotective role to the neurocompensatory response elicited by carotid balloon injury: Consequences on contralateral carotid tone and blood flow. Eur J Pharmacol. 2013. 708:124-138. https://doi.org/10.1016/j.ejphar.2013.02.053
Shen Y, Li CG, Zhou SF, Pang EC, Story DF, Xue CC. Chemistry and bioactivity of Flos Magnoliae, a Chinese herb for rhinitis and sinusitis. Curr Med Chem. 2008. 15:1616-1627. https://doi.org/10.2174/092986708784911515
Shi J, Yang Y, Cheng A, Xu G, He F. Metabolism of vascular smooth muscle cells in vascular diseases. Am J Physiol Heart Circ Physiol. 2020. 319:H613-H631. https://doi.org/10.1152/ajpheart.00220.2020
Singh M, Bacolla A, Chaudhary S, Hunt CR, Pandita S, Chauhan R, et al. Histone acetyltransferase MOF orchestrates outcomes at the crossroad of oncogenesis, DNA damage response, proliferation, and stem cell development. Mol Cell Biol. 2020. 40:e00232-20. https://doi.org/10.1128/mcb.00232-20
Sykes SM, Mellert HS, Holbert MA, Li K, Marmorstein R, Lane WS, et al. Acetylation of the p53 DNA-binding domain regulates apoptosis induction. Mol Cell. 2006. 24:841-851. https://doi.org/10.1016/j.molcel.2006.11.026
Tanaka K, Konno Y, Kuraishi Y, Kimura I, Suzuki T, Kiniwa M. Synthesis of a magnosalin derivative, 4-(3,4,5-trimethoxyphenyl)-6-(2,4,5-trimethoxyphenyl)-2-diethylaminopyrimidine, and the anti-angiogenic and anti-rheumatic effect on mice by oral administration. Bioorg Med Chem Lett. 2002. 12:623-627. https://doi.org/10.1016/s0960-894x(01)00810-1
Wang F, Zhang G, Zhou Y, Gui D, Li J, Xing T, et al. Magnolin protects against contrast-induced nephropathy in rats via antioxidation and antiapoptosis. Oxid Med Cell Longev. 2014. 2014:203458. https://doi.org/10.1155/2014/203458
Wang K, Deng X, Shen Z, Jia Y, Ding R, Li R, et al. High glucose promotes vascular smooth muscle cell proliferation by upregulating proto-oncogene serine/threonine-protein kinase Pim-1 expression. Oncotarget. 2017. 8:88320-88331. https://doi.org/10.18632/oncotarget.19368
Wright JN, Collins HE, Wende AR, Chatham JC. O-GlcNAcylation and cardiovascular disease. Biochem Soc Trans. 2017. 45:545-553. https://doi.org/10.1042/bst20160164